Climate Dynamics (2024) 62:2041–2056
https://doi.org/10.1007/s00382-023-07009-w

ORIGINAL ARTICLE

Diurnal variations of summer rainfall response to large-scale circulations and low-level winds over the Sichuan Basin

Juan Li[1] · Haoming Chen[1,2] · Xingwen Jiang[3,4] · Puxi Li[1,2]

Received: 19 June 2023 / Accepted: 24 October 2023 / Published online: 23 November 2023

Abstract

The evident nocturnal peak dominates the summer rainfall over the Sichuan Basin (SCB), which is closely related to the nocturnal intensification of low-level winds. Based on 21-year IMERG rainfall product and reanalysis data during summertime (June–August) from 2000 to 2020, the low-level winds are classified into four groups, with strong or weak daily mean wind accompanied by a large or small diurnal amplitude, to clarify their influences on rainfall over the SCB. The results show that under strong daily mean wind conditions, the westward extension of the Western Pacific Subtropical High (WPSH) determines the southwesterly monsoon airflow to be tuned to the southerly over the eastern Yunnan-Guizhou Plateau, which provides abundant warm and moist air resources for rainfall within the basin through the southeastern side of the SCB. Strong mean winds, coupled with a large diurnal amplitude due to the acceleration of easterly, strengthen the moisture convergence at night, and contribute to the rainfall increasing remarkable over the SCB with a peak at midnight. Meanwhile, there is an apparent anomalous low-level warming over the SCB, creating more unstable atmospheric conditions. In addition, the weak upward motion associated with the afternoon heating over the eastern slope of the Tibetan Plateau (TP) enhances the easterly and facilitates the development of upward motion over the western SCB in the early night, which is responsible for the larger diurnal amplitude of rainfall. On the contrary, rainfall is suppressed and the diurnal amplitude of rainfall is gentle under the condition of weak daily wind with small diurnal amplitude, due to the weak moisture transport and cooling planetary boundary layer related to the deepened midlatitude trough, as well as more active convection over the eastern slope of TP during the day. The results imply that atmospheric conditions associated with diurnal variation of low-level winds should be considered as a key component in regulating the rainfall and moisture budget over the SCB, the strength of low-level winds in the early evening may provide a predictive signal for the development of nocturnal rainfall over the SCB.

Keywords The Sichuan Basin · Diurnal variation of rainfall · Low-level jet · Tibetan Plateau

1 Introduction

The Sichuan Basin (SCB) in southwest China is located on the east of the Tibetan Plateau (TP), with the Daba and Wu Mountains to the northeast, and the Yunnan-Guizhou Plateau (YGP) to the south (Fig. 1). Influenced by this unique topography, the SCB region suffers from frequent occurrences of heavy rainfall in summer, which often trigger secondary disasters such as landslides and flash floods leading to serious casualties and economic losses, and posing a great challenge to weather forecasting. Moreover, the rainfall over the SCB exhibits strong diurnal variations, and the nocturnal rainfall has been found to account for up to 70% of the total rainfall over the SCB (Zheng et al. 2016).

Previous studies have shown that the diurnal peak of rainfall has a pronounced eastward time lag from the eastern

✉ Haoming Chen
chenhm@cma.gov.cn

1 State Key Laboratory of Severe Weather, & Institute of Tibetan Plateau Meteorology, Chinese Academy of Meteorological Sciences, China Meteorological Administration, Beijing, China

2 Research Center for Disastrous Weather over Hengduan Mountains & Low-Latitude Plateau, China Meteorological Administration, Kunming, China

3 Institute of Plateau Meteorology, China Meteorological Administration, Chengdu, China

4 Heavy Rain and Drought-Flood Disasters in Plateau and Basin Key Laboratory of Sichuan Province, Chengdu, China

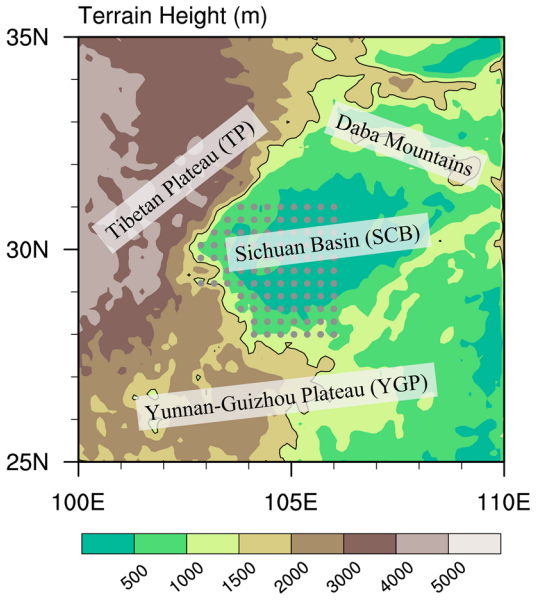

Fig. 1 The terrain height over the SCB and its surrounding areas (unit: m). The black contour is for the 1500 m elevation, and the gray dots indicate the focused areas with large rainfall over the SCB

TP to the SCB, that is, the diurnal peak of rainfall occurs in the early evening over the eastern TP, whereas it occurs at midnight or early morning over the SCB (Yu et al. 2007a; Bao et al. 2011; Jin et al. 2013). Within the SCB, the diurnal variation of rainfall exhibits evident regional features. Rainfall tends to initiate over the southwestern SCB in the early evening and propagate eastward to cover the entire SCB by the early morning (Qian et al. 2015; Li et al. 2021). Summer rainfall over the SCB is mainly the result of the large-scale circulations (such as the Western Pacific Subtropical High (WPSH), the Asian summer monsoon, and troughs in the westerlies) (Ueno et al. 2011; Luo et al. 2020) and the weather systems influenced by the TP (such as the mesoscale Southwest China Vortex, the topography forces the uplift of water vapor) (Xu et al. 2010; Feng et al. 2016; Fu et al. 2019).

Focusing on the diurnal variations of rainfall over the SCB, numerous studies have been carried out to explore the physical mechanisms in controlling the nocturnal rainfall over the SCB from various perspectives. The general view is that the upward branch associated with thermally driven mountain-plain solenoids due to differential heating and cooling between elevated plateaus and basins contributes to the nocturnal rainfall over the SCB (Bao et al. 2011; Jin et al. 2013; Qian et al. 2015). Some studies pointed out the possible role of long wave radiative cooling at the cloud top in enhancing nocturnal rainfall over the SCB (Yu et al. 2007b; Chen et al. 2010). Li et al. (2008) found that the afternoon cloud cover in southwest China leads to unfavorable conditions for afternoon rainfall. Other researchers suggested that the nocturnal rainfall over the SCB may be related to the eastward propagation of convective systems originating over the TP (Hu et al. 2016; Li et al. 2017; Curio et al. 2019). Moreover, convective instability is usually generated in the eastern part of the SCB where the warm moist inflow from south is enhanced at night, it is more supportive to the growth of rainfall episodes in the eastern regions (Chen et al. 2014). Recently, the nocturnal low-level jet (LLJ) related moisture advection is suggested to be more important than the mountain-plain solenoids processes regarding the moisture convergence for nocturnal rainfall over the SCB, the moisture convergence and divergence caused by low-level winds play a more crucial role in modulating the diurnal variation of rainfall over the SCB (Zhang et al. 2019; Li et al. 2021).

It is well realized that the diurnal cycle of low-level winds, in particular the nocturnal acceleration of LLJs, induces low-level convergence at their terminus and results in the diurnal cycle of moisture transport and further regulates rainfall. The enhanced LLJs at night has been observed in many regions worldwide. The inertial oscillation theory associated with the diurnal change in the effect of surface friction on the planetary boundary layer (PBL) (Blackadar 1957) and the terrain thermal forcing theory caused by the diurnal change of the horizontal pressure gradient force due to differential heating and cooling of sloping terrain (Holton 1967) are often combined to explain the diurnal variation of winds, although the Blackadar inertial oscillation theory may have a larger contribution (Shapiro et al. 2016; Xue et al. 2018). The enhanced nocturnal low-level winds also produce the nocturnal rainfall over many regions of China (Yu et al. 2009; Chen et al. 2010). The nocturnal low-level southwesterlies strengthen the moisture transport and generate convective instability by the low-level convergence at the Mei-Yu front, contributing to the development of heavy rainfall in the pre-dawn hours (Zeng et al. 2019; Cui et al. 2023). In addition, the LLJs are well-correlated with local valley wind circulations under stable boundary layer conditions at night, facilitating the nocturnal rainfall over the plains or windward slopes (Sun and Zhang 2012; Pan and Chen 2019; Wang et al. 2023).

In summer, the sensible heated TP acts as a large air pump, driving the large nocturnal acceleration of the monsoon flow, which converges at the windward slopes with anomalous upward motions (Chen 2020). The prominent thermal vertical circulations occur between the eastern TP and the adjacent SCB and YGP. Moreover, the low-level winds show an obvious diurnal change over the SCB, with the easterly nocturnal LLJ dominating the southeastern SCB and the eastern YGP (Zhang et al. 2019; Li et al. 2021). The low-level easterly winds blowing towards the eastern slope of the TP could force ascent by blocking the easterly winds and providing moisture transport, which favor of the

initiation and development of nocturnal convective systems. The contrast in cloud radiative forcing between the elevated plateau and downstream plain also plays a key role in connecting the atmospheric circulations and rainfall systems by influencing the thermal forcing and moisture processes (Stephens 2005; Zeng et al. 2019; Wu and Chen 2021). The diurnal variation of low-level winds as the key factor regulating the diurnal variation of rainfall over the SCB, is affected by thermodynamic/dynamic forcing in the boundary layer and the topography of the TP. Furthermore, the diurnal variation of low-level winds also shows a strong dependence on the mean flows, and varies seasonally with the progress of monsoon circulations. Thus, both the large-scale daily winds and the regional forcing can greatly modulate the regional nocturnal rainfall. Chen (2020), Chen et al. (2021) considered the daily mean flows and diurnal amplitude of the southerly wind over the Asian monsoon region and studied the associated atmospheric circulation, rainfall systems and water vapor budget, as well as the diurnal changes on intraseasonal and interannual scales. However, it is not clear how this diurnal change of winds coupled with mean flows at night affects the diurnal cycle of rainfall over the SCB.

In this study, the low-level winds over the southeastern SCB have been classified into four groups based on the daily mean winds and their diurnal amplitude. The comparison of different circulation conditions and associated rainfall and atmospheric processes may help us to better understand the importance of multi-scale circulation for nocturnal rainfall and provide a promising way to improve the simulation of rainfall over the SCB. The rest of this paper is organized as follows. Section 2 introduces the dataset and methods used in this study. Section 3 describes the climatological relationship between diurnal cycle of rainfall and winds over the SCB. The spatio-temporal evolution of rainfall in response to different atmospheric circulations is shown in Sect. 4. Section 5 examines the detail atmospheric processes governing rainfall associated with different circulation conditions. Finally, conclusions and a discussion are given in Sect. 6.

2 Dataset and methods

a. Dataset used in this study

In this study, the Integrated Multi-satellitE Retrievals (IMERG) for Global Precipitation Measurement (GPM) rainfall product with a spatial resolution of $0.1° \times 0.1°$ and a time interval of 30 min is used to analyze the characteristics of rainfall systems. The GPM mission is the successor of Tropical Rainfall Measuring Mission (TRMM), marking a transition from the TRMM era to the GPM era. The GPM Core Observatory carries a dual-frequency precipitation radar (DPR) and a conical-scanning multi-channel GPM Microwave Imager (GMI), which largely improves the measurement of precipitation (Hou et al., 2014). IMERG is derived from multiple measurements of GPM, including passive microwave, infrared, and radar data. IMERG provides three products, including the early, late and final runs (Huffman et al. 2015). The IMERG final run is calibrated by the monthly Global Precipitation Climatology Centre precipitation gauge analysis (Huffman et al. 2014). The Level-3 IMERG final run product is available since June 2000, and the data in the summer from 2000 to 2020 are analyzed in our study.

The IMERG rainfall product presents well in reproducing regional variations of daily rainfall and the spatial pattern of diurnal cycle of rainfall in mainland China, which resembles rain gauge measurements, it also shows more satisfactory agreement at the daily and hourly time scales for the months of June–September (Tang et al. 2016; Asong et al. 2017). Moreover, the comprehensive analysis on the connections between spatial variations in errors of IMERG rainfall and geographical features in Sichuan Province of China suggested that the increased digital elevation model plays a positive role in reducing the hit bias in the lower regions (< 1.5 km) (Li et al. 2022a, b). Previous studies highlight a potential applicability of IMERG Final Run as a reliable source of precipitation estimates in diverse water resources and hydrometeorological applications.

The latest hourly ERA5 reanalysis data with a horizontal resolution of $0.25° \times 0.25°$, conducted by the European Centre for Medium-Range Weather Forecasts and developed through the Copernicus Climate Change Service, is used to represent the atmospheric conditions in this study (Hersbach et al. 2019). The dataset has been shown to faithfully capture the diurnal variations of winds and other variables, and is widely used to represent the circulation conditions over the TP and surrounding areas (Hu et al. 2020; Sun et al. 2021).

All datasets used in this study cover June–August from 2000 to 2020. As the diurnal cycle of low-level atmospheric general circulation is usually regulated by boundary layer heating during the day (Xue et al. 2018; Chen 2020), the diurnal cycle is estimated from 13:00 LST to following 12:00 LST. The diurnal deviations of all variables are obtained by subtracting the daily mean, and the anomalies are the difference from the 21-year climatological mean.

b. Methods

In this study, to clarify the processes that govern the rainfall over the SCB, the daily mean wind speed and the diurnal deviation wind at 20:00 LST of 850 hPa over the southeastern SCB are used to represent the intensities of the daily mean wind and its diurnal amplitude, respectively. Our previous study suggested that the diurnal deviation of easterly wind at 20:00 LST plays an important role in the

initiation of rainfall over the SCB (Li et al. 2021), the intensity of easterly deviation wind may contribute greatly to the nocturnal rainfall over the SCB. To get a more optimal selection of wind variables and domains, the regression patterns of rainfall and horizontal wind at 850 hPa regressed onto the standardized daily rainfall at the western SCB (the region as gray dots in Fig. 1) are shown in Fig. S2. Positive rainfall anomalies are observed over the SCB, with the maximum value reaching more than 14 mm day^{-1} at the western SCB (Fig. S2a). Accordingly, the cyclonic circulation over the SCB is associated with the southwesterly monsoon flow to the south, and turns to southerlies or southeasterlies entering the SCB through its southeastern boundary. Over the southeastern SCB, the zonal wind component at 850 hPa has a maximum positive correlation with the rainfall over the SCB, indicating that the changes of zonal wind are tied to the rainfall. Furthermore, the regression patterns of rainfall diurnal difference and diurnal deviation wind suggest that the nocturnal rainfall over the SCB is also tied to the easterly deviation wind at early evening (Fig. S2b). Therefore, such a selection of low-level wind at both daily and diurnal time scales can well measure their effect on rainfall over the SCB. At the daily time scale, a strong (weak) background wind is defined when the daily mean wind speed over the southeastern SCB at a given day is above (below) the climate mean (5.33 m s^{-1}) during the summer from 2000 to 2020, named D(+) and D(–) days, respectively. At the diurnal time scale, the A(+) days denote the days with large diurnal amplitudes when the diurnal easterly deviation at 20:00 LST on a given day is above the climate mean deviation (– 1.39 m s^{-1}). The remaining days are considered as the days with small diurnal amplitudes, named A(–) days.

Based on this definition, a total of 1932 summer days can be grouped into four categories. The strong daily mean wind days with large diurnal amplitudes are designated D(+)A(+), while those with small diurnal amplitudes are D(+)A(–). Similarly, the weak daily mean wind days with large diurnal amplitudes are designated D(–)A(+), while those with small diurnal amplitudes are D(–)A(–). Figure 2 shows the scatterplots of the diurnal deviation of zonal wind at 20:00 LST with daily-mean wind speed and with the diurnal deviation of meridional wind at 02:00 LST over the southeastern SCB. As a result, the diurnal zonal deviation wind at 20 LST is correlated with the daily mean wind speed, with a correlation coefficient of – 0.41 over the southeastern SCB (Fig. 2a). The occurrence of D(+)A(+) days is more than twice that of D(+)A(–) days, and the occurrence of D(–)A(–) days is about 1.7 times that of D(–)A(+) days. This indicates that the large (small) diurnal variations of low-level wind tend to occur in the strong (weak) mean wind condition (Shapiro et al. 2016; Chen 2020). Furthermore, the zonal easterly component at early evening exhibits a well correlation with the meridional southerly component at midnight, which coincides with the diurnal peak of rainfall over the SCB, with a correlation coefficient of – 0.65 (Fig. 2b), implying that the diurnal southerly deviation wind governed by the inertial oscillation also should be considered as an important role controlling the nocturnal rainfall

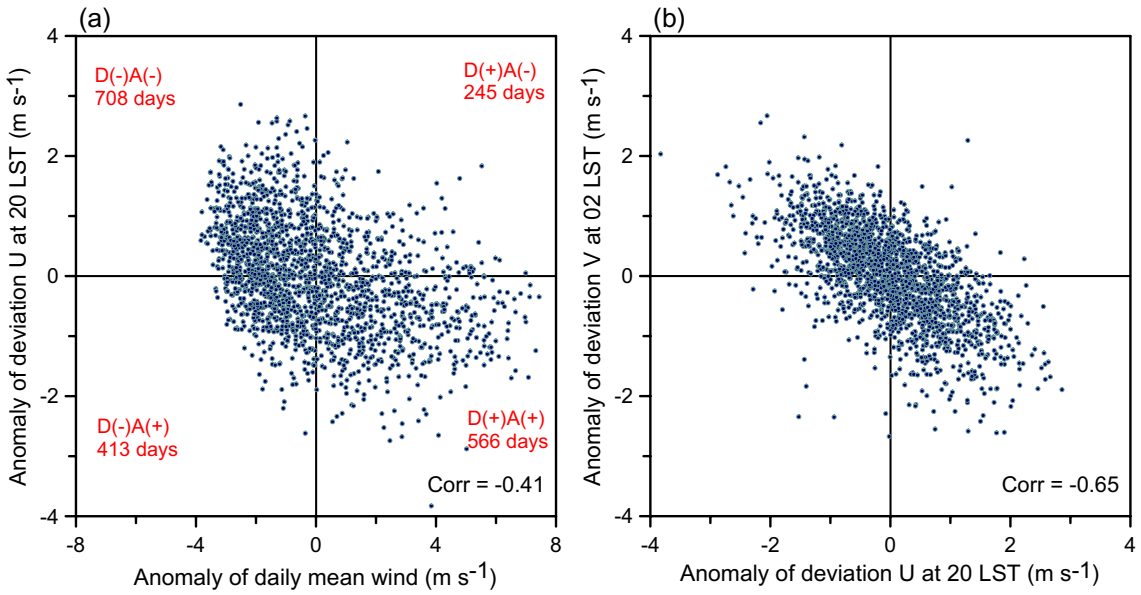

Fig. 2 Scatterplots of the diurnal deviation of zonal wind at 20:00 LST with daily-mean wind speed (**a**) and with the diurnal deviation of meridional wind at 02:00 LST (**b**) over the southeastern SCB (outlined in Fig. 3). The anomalies are the difference from the climatological mean. The occurrence days of four different conditions are marked in (**a**). The correlation coefficient of two variables is shown at the right bottom of each figure

over the SCB. The same method has been used to study the East Asian summer monsoon rainfall (Chen 2020; Liu et al. 2022). It is worth noting that the southeastern SCB, which we focus on in this study, is a region with large diurnal amplitude compared to the eastern China (figure not shown). Thus, the comparison among these four groups is helpful to understand the influence of different couplings of the multi-scale atmospheric circulation and their diurnal variations on rainfall over the SCB.

In this study, the diurnal amplitude of rainfall is calculated as:

$$A = \frac{P_{\max} - \overline{p}}{\overline{p}},$$

where A is the diurnal amplitude of rainfall, P_{max} is the maximum of hourly rainfall in one day, and $\overline{P}$ is the daily mean rainfall (Yuan et al. 2013).

3 Climatology of the diurnal cycles of rainfall and low-level winds over the SCB

a. Spatial distributions of rainfall and associated low-level winds

Figure 3 shows the spatial distributions of the normalized amplitude of diurnal variations of rainfall and the daily mean 850-hPa winds, as well as the zonal deviation winds at 20:00 LST over the SCB and surrounding areas during the summer. Within the SCB, the spatial distributions of the normalized amplitude of diurnal variations of rainfall are similar to that of climatological rainfall (Fig. S1), the rainfall exhibit large amplitude over the eastern TP and southwestern SCB, with the maximum hourly rainfall exceed 1.2 times of the daily mean rainfall. From the daily mean 850-hPa winds, we can see that there is a strong southeasterly flow into the SCB from the southeastern side of the SCB, which clearly brings warm and moist air from the lower latitudes of the ocean into the basin, and also creates anomalous convergence that favors rainfall. Moreover, the diurnal deviation of zonal wind shows a large diurnal amplitude over the southeastern SCB (purple contours in Fig. 3), indicating that significant diurnal variations of low-level winds play an important role in regulating diurnal variations of summer rainfall over the SCB, which is the focus of this study.

Figure 4 shows the averaged diurnal cycles of the summer rainfall and low-level winds over the SCB, every 3-h starting at 14:00 LST. From noon to afternoon, the rainfall first develops over the eastern slope of the TP, with considerable rainfall observed at 17:00–20:00 LST. At these hours, the rainfall is suppressed over the SCB, with the central part of the SCB largely free of rainfall. The terrain-dependent

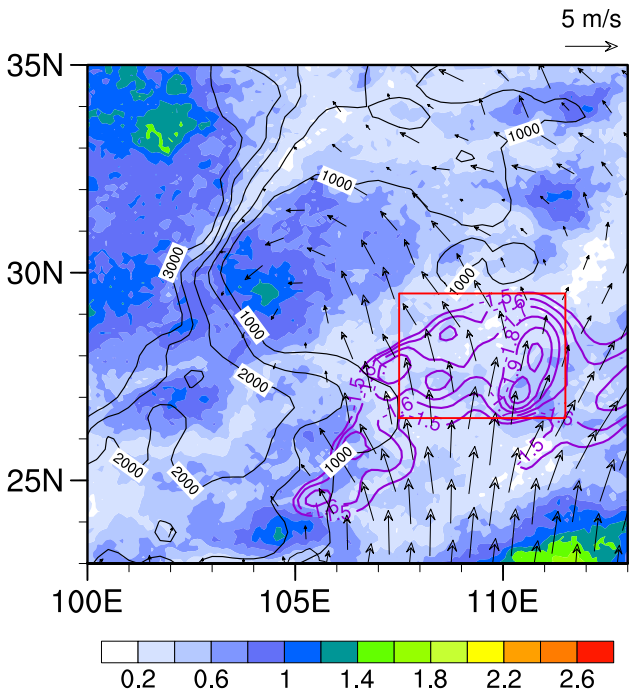

Fig. 3 Spatial distributions of diurnal amplitude (normalized by the daily mean) of rainfall (shading) and daily mean 850-hPa winds (vectors, unit: m s^{-1}), as well as the diurnal deviation of the zonal wind at 20:00 LST (removing the daily mean, purple contours for less than – 1.5 m s^{-1}) during the summer from 2000 to 2020. The black contours indicate the terrain height at 500 m intervals, and the red box marks the southeastern SCB region

features reveal a strong influence of thermal contrast due to daytime heating (Yuan et al. 2012; Chen 2020). In the early night (20:00 LST), rainfall has started along the southwestern SCB, mostly along the steep terrain from the eastern TP to the SCB. The rainfall then develops and extends to the northeast, covering the entire basin at 02:00 LST. The spatial distributions of rainfall at night resemble well the daily mean patterns (figure not shown), suggesting that the night rain systems contribute greatly to the total rainfall amount. After midnight and through the early morning hours, the rainfall weakens and retreats to the northeastern half of the SCB. In addition, the prevalent nocturnal rainfall area over the western SCB is also prone to frequent heavy rainfall events at night (Zhao 2015; Xia et al. 2021).

In terms of the 850-hPa winds (the red vectors in Fig. 4), in general, basically cyclonic circulation is evident throughout the day over the SCB. The cyclonic convergence gets strong at 20:00 LST, and peaks at midnight. Consequently, the stronger southerly flow brings more moisture into the SCB, and the heaviest rainfall is found near this time over the basin. Given the daily mean winds, the diurnal deviation of 850-hPa winds is obtained by subtracting the daily mean value (the black vectors in Fig. 4). It is noticeable that the deviation of 850-hPa wind exhibits a clockwise

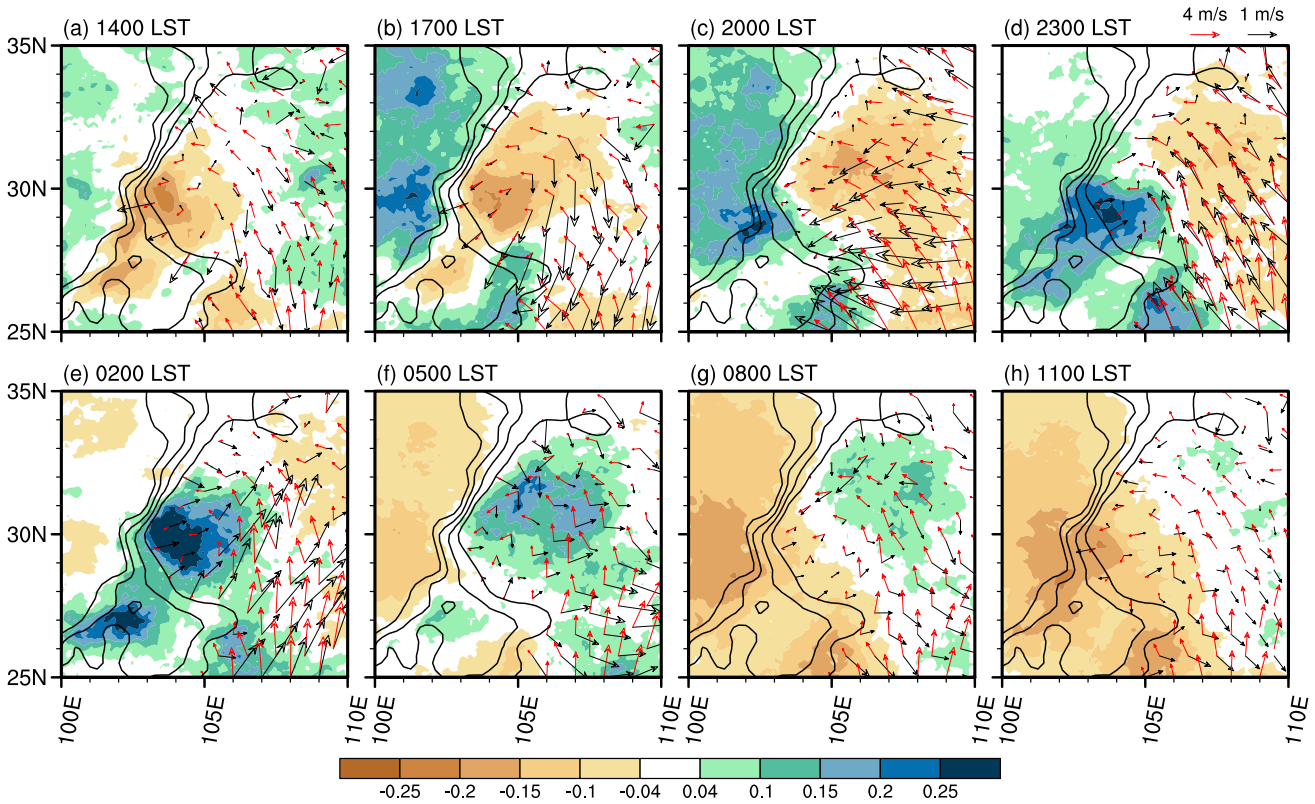

Fig. 4 Diurnal deviation of summer rainfall (shading, unit: mm h^{-1}), original 850-hPa winds (red vectors, unit: m s^{-1}) and their deviation (black vectors, unit: m s^{-1}) derived by subtracting the daily mean from 2000–2020. The black contours indicate the terrain height at 500 m intervals

diurnal rotation, changing from easterlies in the early evening (Fig. 4c) to mostly southerlies in the midnight (Fig. 4d, e), which contributes to the diurnal peak of rainfall, and then to westerlies (Fig. 4f, g) in the early morning and northerlies in the early afternoon (Fig. 4a, b). Such clockwise rotation of deviation wind vectors largely attributed to the diurnal inertial oscillation of boundary layer friction as explained by the Blackadar (1957). In the early evening, the prevailing easterly deviation winds flow into the basin from the southeastern side of the SCB, and is convergent over the eastern slope of the TP that contributing to the initiation of rainfall over the southwestern SCB (Fig. 4c). While the westerlies and the northerlies pull the most air out of the SCB, and result in divergence that suppressing rainfall during the day. This indicates that the low-level winds and their diurnal changes over the southeastern SCB play an important role in modulating the rainfall within the SCB.

We further examine the relationship between the diurnal changes of 850-hPa winds over the southeastern SCB and the diurnal rainfall over the focused region (shown as gray dots in Fig. 1). Figure 5a shows that the diurnal wind speed peaks at 23:00 LST, which is about 3 h before rainfall peak at 02:00 LST. Meanwhile, the diurnal deviation of zonal wind increases in the afternoon, and is strongest at 20:00 LST, corresponding to the initiation of rainfall. The deviation of zonal wind gradually decreases and changes to the westerly wind at 01:00 LST. Such disturbance flows enhance nocturnal rainfall at 02:00 LST and suppress rainfall during the day. In order to investigate the influence of low-level winds on the diurnal variations of rainfall over the SCB, we analyze the vertical structure of winds over the southeastern side of the basin (Fig. 5b, c). It can be seen that both the daily mean (Fig. 5b) and diurnal deviation winds (Fig. 5c) have a prominent LLJ with the maximum wind speed at about 850 hPa. In the early afternoon at 14:00 LST, the zonal wind is weaker, which is probably due to the intense vertical mixing within the boundary layer according to Blackadar theory (Blackadar 1957). The boundary layer jet can enhance the most important moisture supply for rainfall within the SCB, and the diurnal variations of the easterly LLJ play the more important role in controlling the diurnal cycles and especially the maximum of rainfall shortly after midnight over the SCB. This indicates that the atmospheric conditions associated with the low-level winds should be considered as a key factor affecting rainfall over the SCB, which inspires a detailed analysis below.

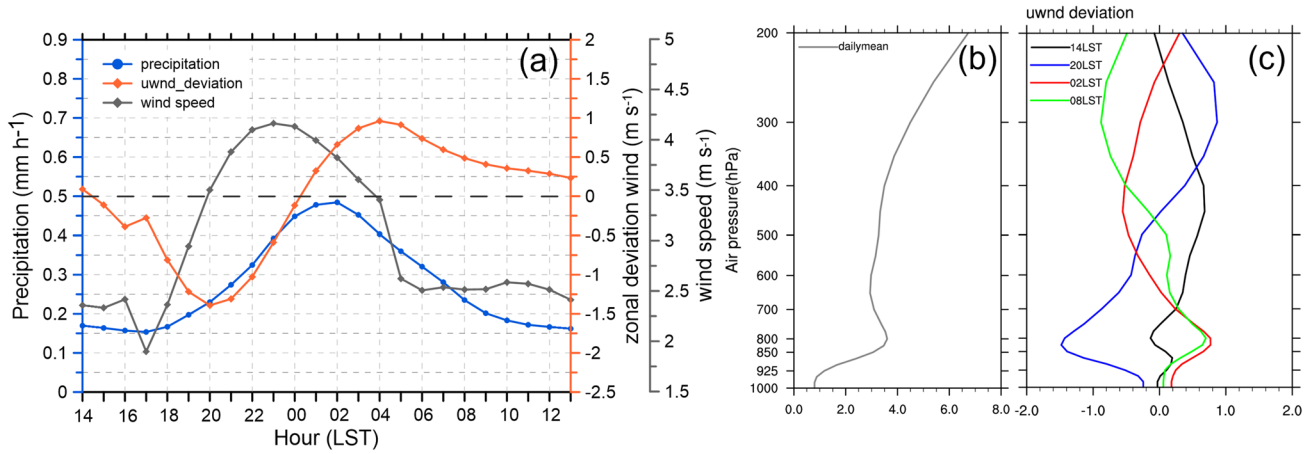

Fig. 5 **a** Diurnal variation of mean wind speed and zonal deviation wind (removing the daily mean) at 850 hPa over the southeastern SCB (outlined in Fig. 2) and the diurnal variation of rainfall over the focused region of the SCB (gray dots depicted in Fig. 1). **b** Vertical profile of the daily mean horizontal wind speed averaged over the southeastern SCB. **c** Diurnal variation of vertical profiles of the zonal deviation wind averaged over the southeastern SCB during the summer from 2000 to 2020

b. Diurnal cycle of low-level winds under four different circulation conditions

To give a more direct view of the diurnal variation of the deviation winds, the diurnal variations of 850-hPa zonal deviation winds and the hodograph of the mean deviation wind vectors over the southeastern SCB under four different circulation conditions are shown in Fig. 6. Similar to the climatological mean state, the zonal deviation winds of the four conditions all show a distinct diurnal variation (Fig. 6a), with the easterly deviation winds get strongest at 20:00 LST and the westerly deviation winds get strongest in early morning. The diurnal variation of zonal deviation winds is also most pronounced in the presence of strong mean wind (D(+)A(+)). From the hodograph (Fig. 6b), we can see that the deviation wind vectors show clockwise rotation except for the days in D(–)A(–), a behavior that is again consistent with the Blackadar boundary layer inertial oscillation theory for boundary layer LLJ. In the early night (about 20:00 LST) to midnight, the deviation winds blow directed into the basin, such strong disturbance winds provide most moisture transported into the basin as well as produce boundary layer flow convergence when the moist air encounters the eastern slope of TP. On the contrary, during the day, the wind vectors are directed out of the SCB across its southeastern side, creating low-level flow divergence that responsible for rainfall minimum during the day. As a result, stronger diurnal easterly deviation winds contribute to the larger nocturnal rainfall

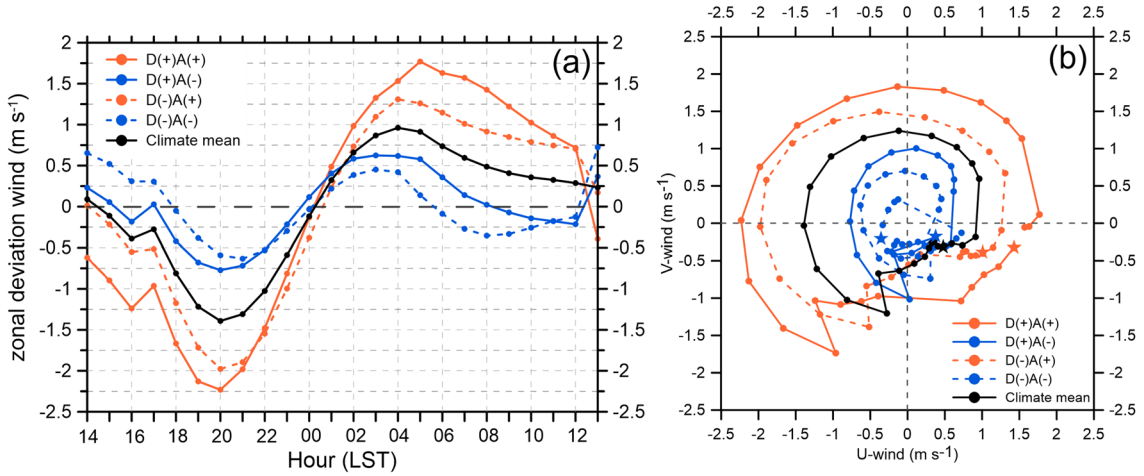

Fig. 6 Diurnal variations of mean zonal deviation winds (removing the daily mean, **a**) and hodograph of hourly deviation winds starting at 08:00 LST (as depicted by the pentagram, **b** at 850 hPa over the southeastern SCB under four different circulation conditions

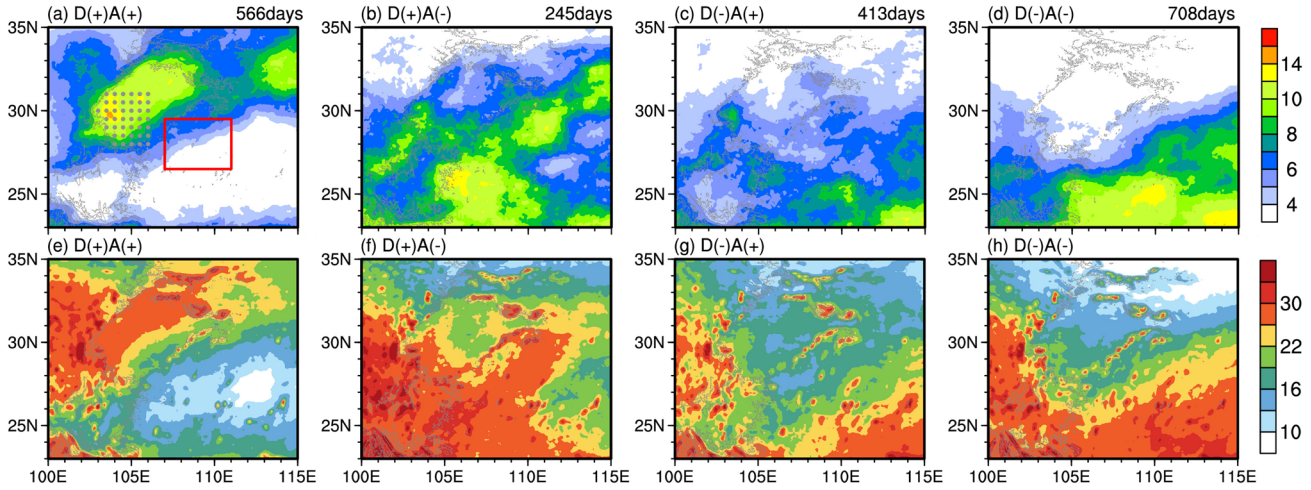

Fig. 7 Spatial distributions of daily mean rainfall amount (**a**–**d**, unit: mm day^{-1}) and rainfall frequency (**e**–**h**, unit: %) under four circulation conditions during the summer from 2000–2020 derived from IMERG. The gray dots indicate the focused areas with large rainfall over the SCB, and the red box marks the southeastern SCB region. The black thin contour is for the 1500 m elevation

over the SCB, and even with weak mean wind, the nocturnal rainfall amount with large diurnal variation is also comparable with the days in D(+)A(–) (Fig. 8). Meanwhile, the diurnal deviation of southerly wind at midnight also exhibits stronger diurnal variations under large diurnal amplitude of zonal deviation wind conditions, which is consistent with the large diurnal amplitude of rainfall over the SCB. These indicate that such flow changes modulate the diurnal cycles of rainfall over the SCB, with the large diurnal amplitude of easterly enhancing the rainfall over the western SCB.

4 Spatiotemporal evolutions of diurnal rainfall in response to different low-level winds

The above analyses imply that the daily mean cyclonic circulation and the diurnal deviation of low-level easterly over the southeastern SCB are closely tied to the nocturnal rainfall over the SCB. The spatial patterns of composite daily mean rainfall and rainfall frequency under four circulation conditions are shown in Fig. 7. In general, more abundant rainfall tends to occur over the SCB and surrounding areas under a strong mean wind condition (Fig. 7a, b). By comparing Fig. 7a, b, it is also evident that the spatial distributions of rainfall have a regional difference over the SCB under the strong mean wind with different diurnal amplitudes. The heavy rain band is concentrated along the western edge of the basin by southwest-northeast orientation on days with the strong mean wind at a large diurnal amplitude (Fig. 7a), which accounts for more than 50% of the summer rainfall within the basin (figure not shown). On the other hand, rainfall is relatively scattered on days with small diurnal

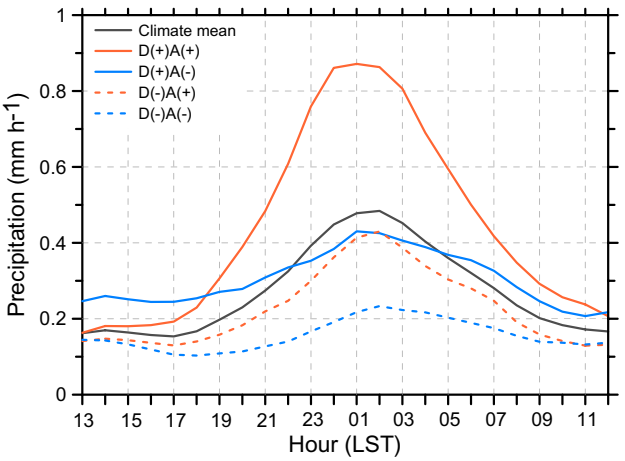

Fig. 8 Diurnal variations of hourly rainfall averaged over the western SCB (as gray dots in Fig. 7a) obtained from IMERG during the summer from 2000 to 2020

amplitude (Fig. 7b), and the rainfall frequency is lower over the SCB (Fig. 7f). As for the weak mean wind (Fig. 7c, d), the rainfall is mostly confined to the south of the basin, and less rainfall is observed over the SCB. In addition, the rainfall remains a slight increase in D(–)A(+) compared to D(–)A(–) over the western SCB, indicating the influence of diurnal easterlies on regional rainfall.

Figure 8 shows the diurnal variations of rainfall averaged over the western SCB under four different atmospheric conditions. In general, the diurnal variations of rainfall under four conditions are similar to that of climate mean state, showing obvious nocturnal rainfall peaking at 01:00–02:00 LST. It is evident that the diurnal variation of rainfall is most pronounced on D(+)A(+) days, which have

strong mean wind coupled with large diurnal amplitude. In addition, the rainfall of large diurnal amplitude with suppressed mean wind also shows more pronounced diurnal amplitude compared to that under conditions of weak diurnal variation. Notably, the rainfall in afternoon hours under D(+)A(+) conditions is weaker than that under D(+)A(–), implying that the associated cloudy condition in the daytime may lead to a small diurnal variation of low-level winds (Chen 2020), which will be discussed in Sect. 5.

The different features of rainfall among four circulation conditions suggest that not only the mean wind can affect the large-scale spatial distribution and intensity of rainfall, but also its diurnal cycle strongly modulates the regional features, highlighting the importance of diurnal variations of low-level winds in the regional climate over the SCB. Since the rainfall mainly occurs under the condition of strong mean wind, we further work on the D(+)A(+) and D(+)A(–) conditions to understand the roles of different diurnal variations under the strong mean wind over the SCB.

5 Atmospheric processes governing rainfall associated with different low-level winds

a. Large-scale atmospheric circulations

We first examine the daily mean low-level winds and their diurnal variations under four different conditions. Figure 9 shows the daily mean 850-hPa winds and relative vorticity, as well as the diurnal amplitude of the 850-hPa zonal wind at 20:00 LST. With strong daily mean wind (Fig. 9a, b), southerly winds prevail over the southeastern SCB and the eastern YGP. The cyclonic circulation over the SCB is associated with the southwesterly monsoon flow to the south, which provides the major moisture supply from the Bay of Bengal and the Indian Ocean, and is tuned to southerly or southeasterly entering the SCB through its southeastern boundary. Thus, considerable rainfall occurs within the SCB, with much more rainfall being displaced to the western SCB at a large diurnal easterly wind over the southeastern SCB (Fig. 7a). Meanwhile, the larger relative vorticity is favorable for larger rainfall over the SCB (Fig. 9a). With weak daily

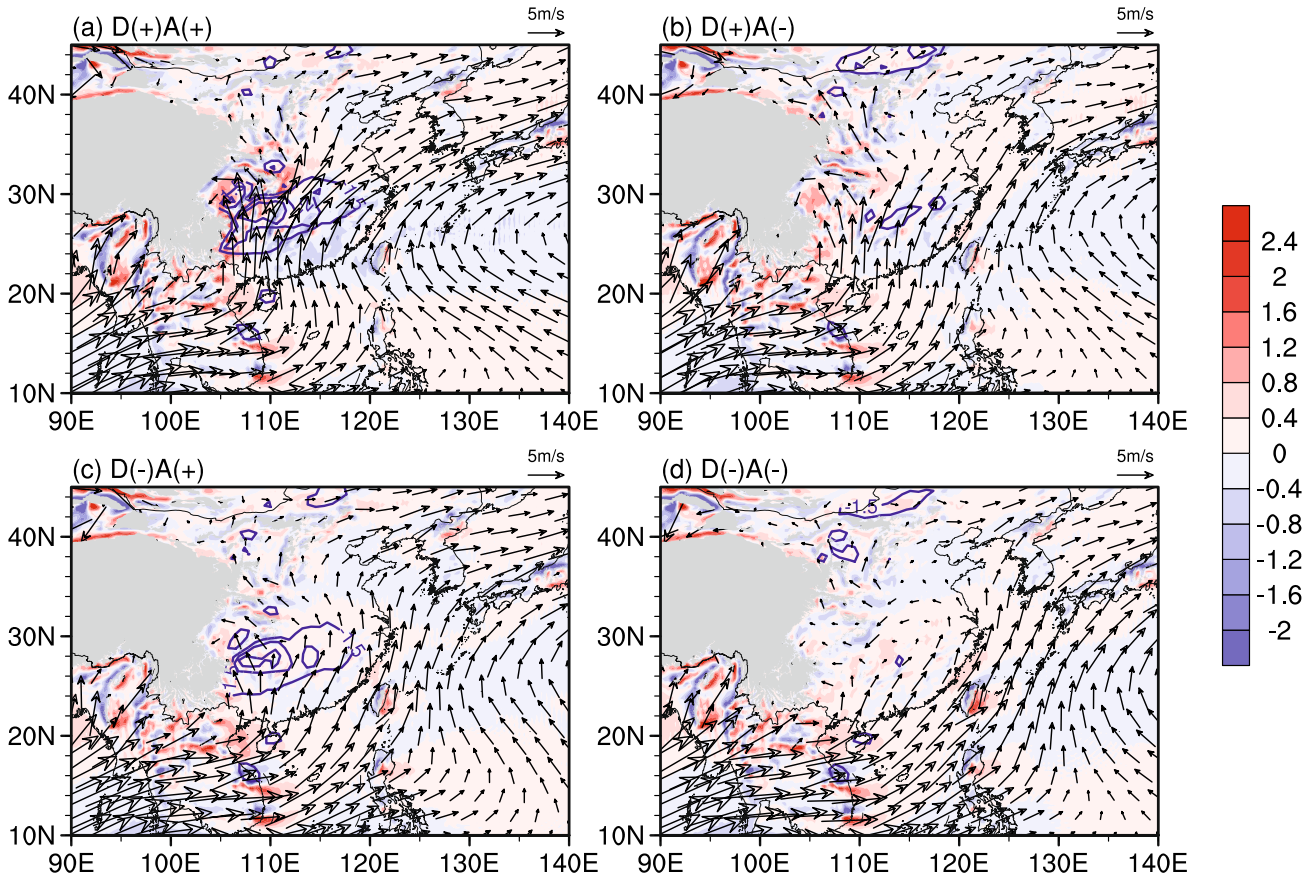

Fig. 9 Composites of daily mean 850-hPa winds (vectors, unit: m s^{-1}) and relative vorticity (shading, unit: 10^{-5} s^{-1}), as well as the diurnal deviation (removing the daily mean) of the zonal wind at 20:00 LST (blue contours for less than – 1.5 m s^{-1}) under four different atmospheric conditions. The gray shading denotes the terrain height above 1500 m

mean wind (Fig. 9c, d), southwesterly monsoon flow over the eastern YGP has a weaker southerly component, and the more warm and moist air is transported to the South China, which contributes to the rainfall there (Fig. 7c, d). On the contrary, the rainfall is suppressed over the SCB on weak mean wind days, and litter rainfall occurs over the western SCB with a large diurnal variation (Fig. 9c).

Figure 10 further examines the large-scale atmospheric conditions at 500 hPa as well as the low-level thermal conditions. With strong mean wind (Fig. 10a, b), the WPSH intensifies and extends westward, reaching the coast of South China, with an anomalous high growing over the eastern China. With weak mean wind (Fig. 10c, d), the WPSH is confined to the 135°E. The location of the WPSH determines the reversal of southwesterly monsoon airflow to southerly over the eastern YGP, which provides abundant warm and moist air resources for rainfall over the SCB on strong mean wind days. When the daily mean wind experiences a large diurnal variation, the westward extension of the WPSH produces anomalous low-level warming over the SCB (Fig. 10a, c), which favors the enhancement of the diurnal amplitude of wind. While a negative low-level temperature anomaly is observed on days with small diurnal amplitude by the deepening midlatitude westerly trough (Fig. 10b, d), the anomalous cooling suppresses the diurnal variations of wind. The low-level thermal condition is thus an important factor influencing the diurnal amplitude of low-level winds. Such warm low-level conditions and apparent ambient winds are conducive to a high occurrence of large diurnal cycles (Fig. 10a) accompanied by active rainfall over the SCB. In addition, the strong southerly transports the relatively warmer air mass from the southeastern edge of the YGP to the SCB during the day, and the accumulation of this anomalous low-level warm air mass can easily cause the atmosphere to become more unstable at night, contributing to the nocturnal peak of rainfall. These different large-scale conditions correspond to the different regional thermal forcing, which further regulates the diurnal variations of rainfall in terms of regional differences and magnitude.

b. Water vapor transport

To investigate the role of the circulations in driving water vapor transport over the SCB, Fig. 11 shows the daily mean water vapor flux and its divergence, as well as the precipitable water anomaly for the four conditions. With strong mean wind (Fig. 11a, b), the daily mean water vapor flux is obviously larger than that of weak mean wind. The differences

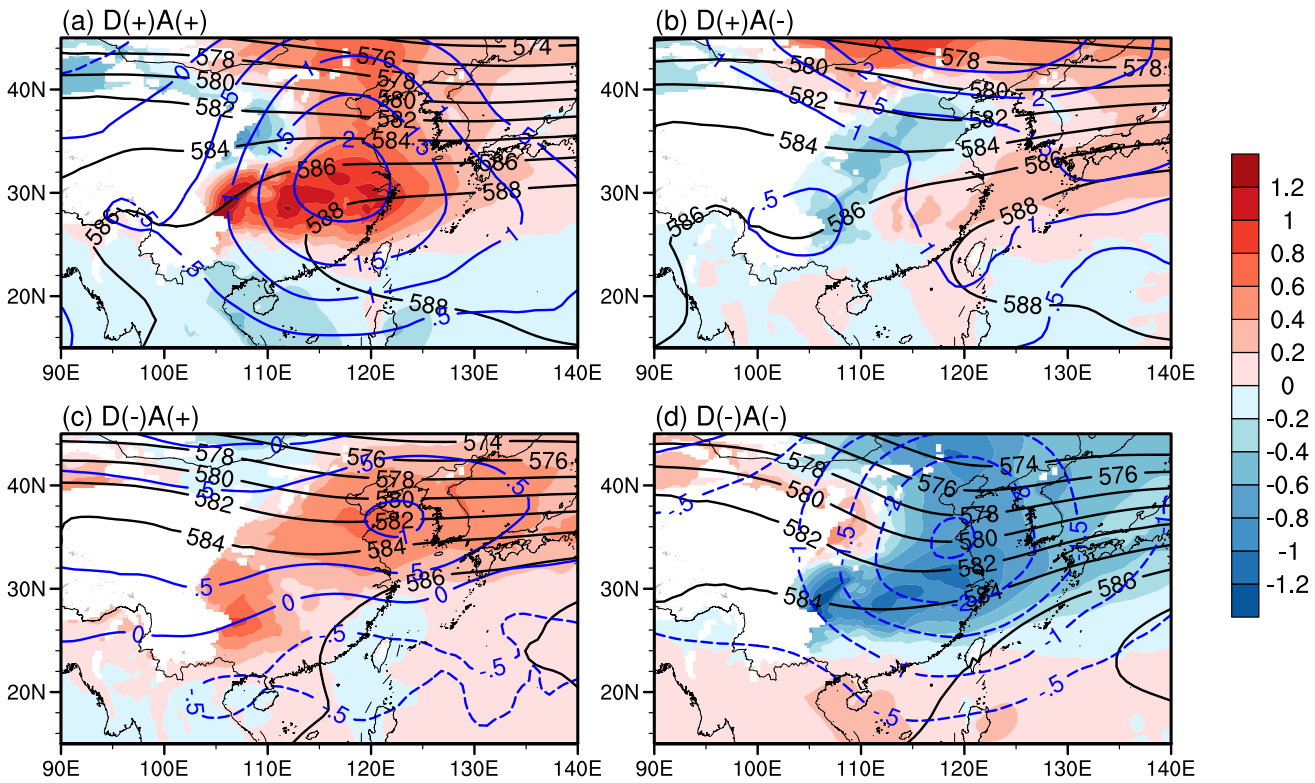

Fig. 10 Composite of 850-hPa anomalous temperature (difference from the 21-year climatological mean, shading, unit: K), 500-hPa geopotential height (black contours, unit: dagpm) and its anomaly (difference from the 21-year climatological mean, blue contours, unit: dagpm) under four different circulation conditions

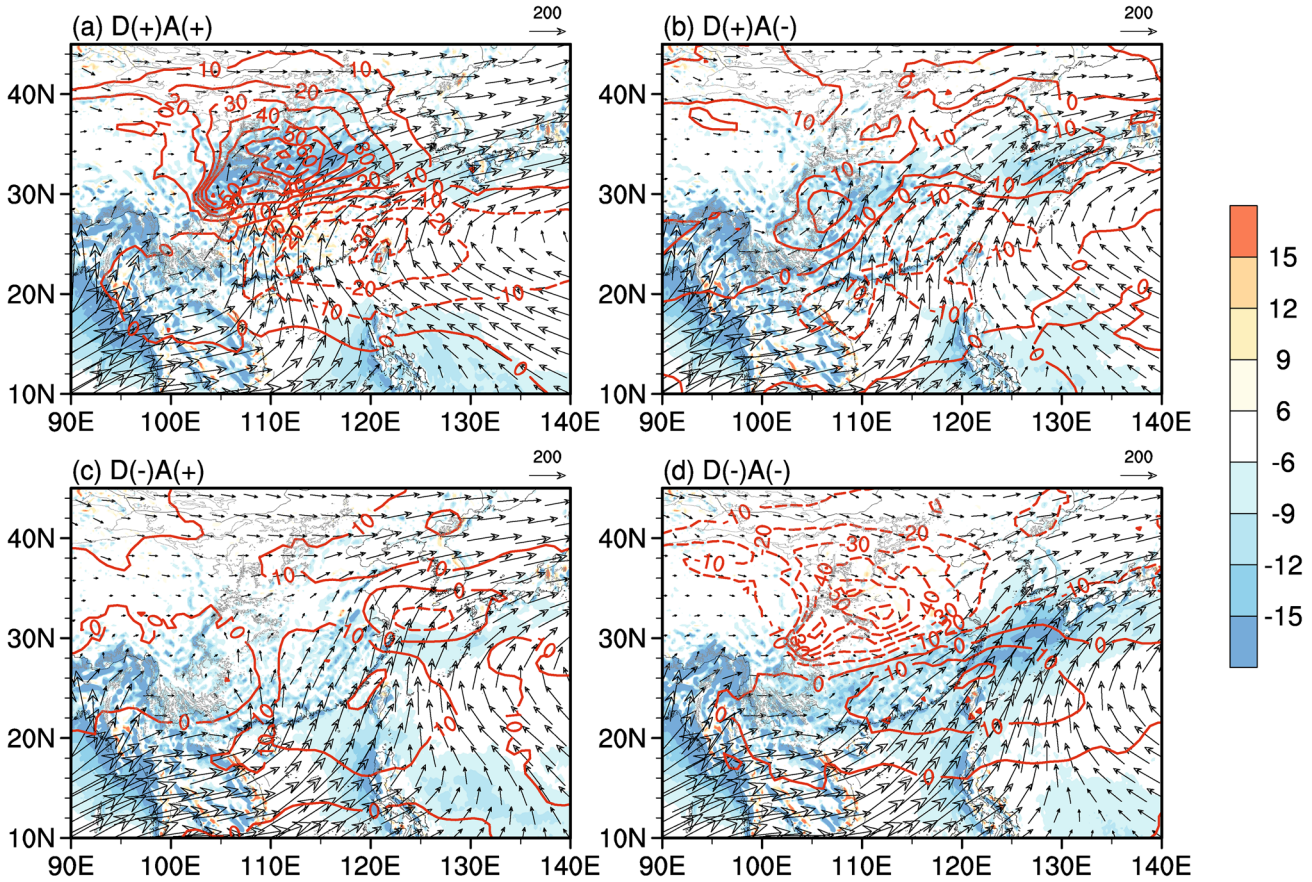

Fig. 11 Composites of daily mean vertical column-integrated moisture flux (integrated from surface to 300 hPa, vectors, unit: kg m^{-1} s^{-1}) and its divergence (shading, unit: 10^{-5} kg m^{-2} s^{-1}), the anomaly (difference from the 21-year climatological mean) of precipitable water (contours, unit: kg m^{-2}) under four different circulation conditions. The black thin contour is for the 1500 m elevation

are mainly caused by the spatial patterns of atmospheric circulation related to the WPSH. The large moisture flux on days with strong mean winds originates from the Bay of Bengal and the Indian Ocean at low latitudes, and the southwesterly moisture transport tunes to the southerly transport over the eastern YGP, where it brings a large amount of warm moist air into the SCB regulated by the westward extension of the WPSH. On days with strong mean wind and a large diurnal amplitude (Fig. 11a), the moisture transport exhibits a cyclonic convergence within the SCB, with the center of moisture flux convergence is located at the western SCB where a distinct wet tongue is observed in terms of the precipitable water anomaly. In comparison, the daily mean moisture flux is much smaller and the moisture from low latitudes southwesterly monsoon is transported to eastern China along the western edge of the WPSH when the southeastern SCB experiences a weak mean wind (Fig. 11c, d). There is an almost negative anomaly of precipitable water throughout the basin, suggesting that the water vapor transport is strongly associated with the evolution of large-scale WPSH.

Figure 12 further examines the diurnal variations of column-integrated moisture flux convergence and precipitable water averaged over the large rainfall region (as gray dots in Fig. 1) of the SCB. In general, the column-integrated moisture flux convergence and precipitable water are larger on days of strong mean wind than those of weak mean wind. Given the large diurnal amplitude (Fig. 12a), the moisture flux convergence increases notably from early night (19:00 LST) to midnight (00:00 LST) and peaks at 21:00 LST (~ -28×10^{-5} kg m^{-2} s^{-1}), which is ~ 4 h earlier than the peak of nocturnal rainfall (Fig. 8). Accordingly, the abundant precipitable water persists during the night hours, with a relatively high daily mean value. Comparing the D(+)A(–) and D(–)A(+) scenarios (Fig. 12b, c), the daily mean moisture flux convergence of D(+)A(–) is greater than that of D(–)A(+), but moisture flux convergence in the days of D(–)A(+) undergoes a more pronounced diurnal cycle, with enhanced nocturnal moisture flux convergence peaking at 21:00 LST, corresponding to the large diurnal cycle of precipitable water. In contrast, the nocturnal increase of moisture flux convergence and precipitable water is less evident

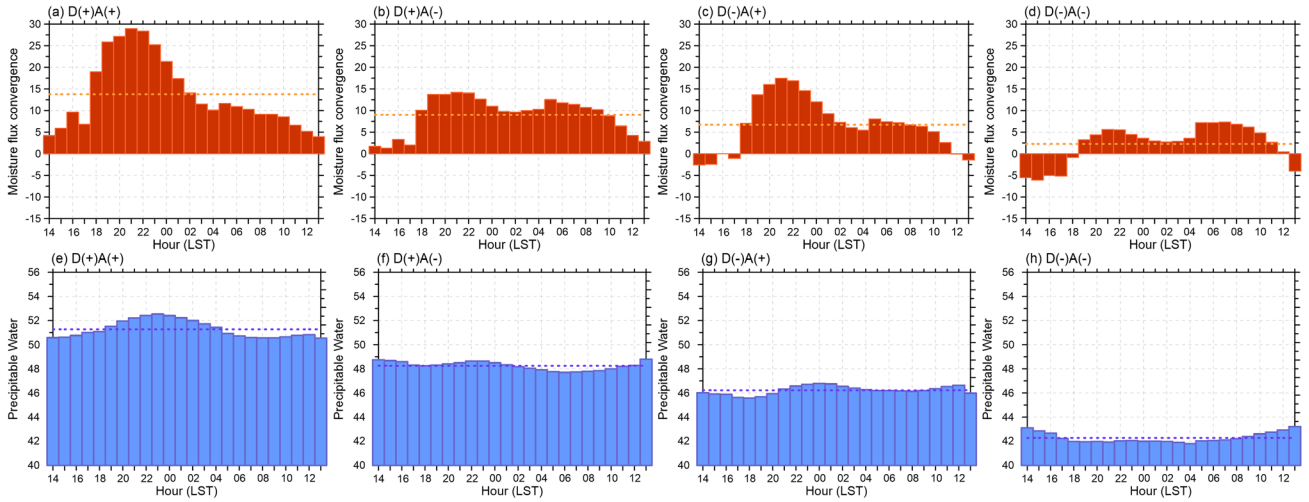

Fig. 12 Diurnal variations of the averaged column-integrated moisture flux convergence (**a**–**d**, unit: – 10^{-5} kg m^{-2} s^{-1}) and precipitable water (**e**–**h**, unit: kg m^{-2}) over the large rainfall region of the SCB as gray dots depicted in Fig. 1 under four different circulation conditions. The dashed lines denote the daily means

over the SCB due to a small diurnal cycle of easterly deviation winds (Fig. 12b, d, f and h). Therefore, the diurnal easterly deviation winds are expected to increase the moisture flux to the SCB in the early night, resulting in a midnight peak in rainfall.

Overall, the strong mean winds coupled with large diurnal variations can significantly affect the water vapor transport over the SCB, and it becomes more efficient at night in regulating the regional moisture budget on a sub-daily time scale. Previous studies have also revealed that nocturnal low-level jets associated with boundary layer inertial oscillations can enhance the moisture transport and low- level convergence, and contribute most to the formation of nocturnal rainfall over East Asia or basins (Zhang et al. 2019; Chen 2020).

c. Vertical motion and atmospheric instability

Focus on the role of strong mean wind with different diurnal amplitude in rainfall over the SCB, Fig. 13 shows the diurnal variations of deviation zonal circulation and vertical motion, as well as the vertical structure of anomalous equivalent potential temperature averaged between 28°N and

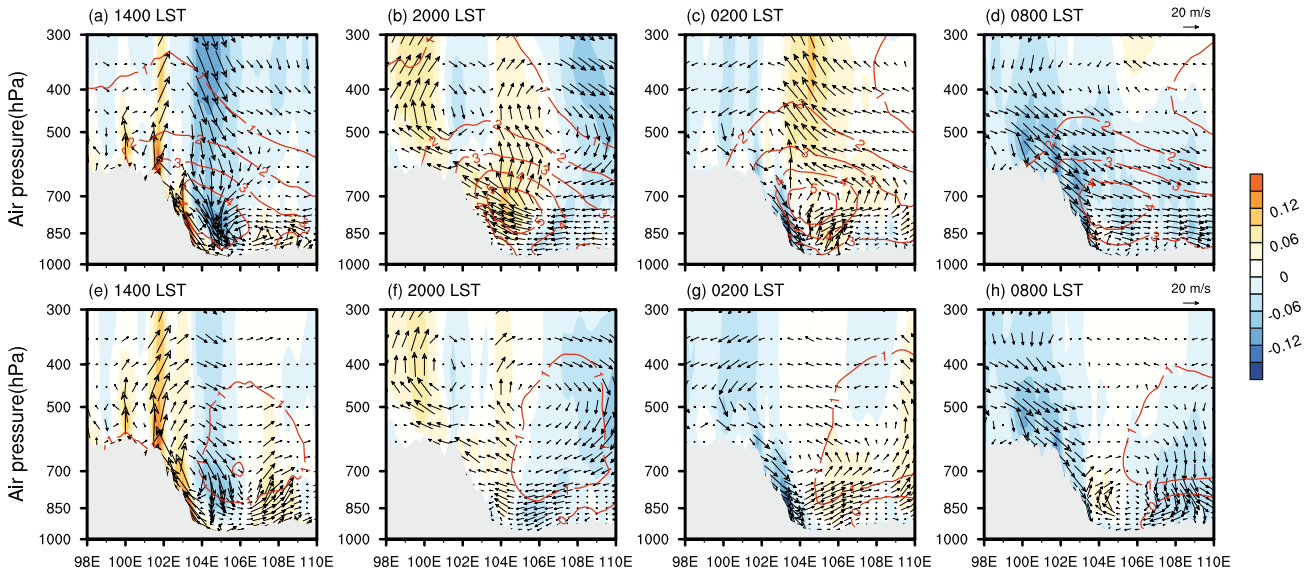

Fig. 13 Diurnal deviations (removing the daily mean) of longitude-vertical circulation (vectors, zonal wind in m s^{-1} and vertical velocity in Pa s^{-1} multiplied by – 400 times) and of vertical motion (shading, unit: – 1.0 Pa s^{-1}) averaged between 28° and 32° N under D(+)A(+) (**a**–**d**) and D(+)A(–) (**e**–**h**) circulation conditions. The red contours denote the anomaly (difference from the climatological mean) of equivalent potential temperature (unit: K)

32°N under D(+)A(+) and D(+)A(–) circulation conditions. As is generally assumed, thermally driven diurnal variations of vertical solenoidal circulations due to the differential diabatic heating and cooling of elevated terrain greatly contribute to the diurnal cycle of rainfall over the eastern TP and the SCB. At 14:00 LST (Fig. 13a, e), the TP is a heat source and the strong upward branch over the eastern slope of the TP produces a favor environment for the convective rainfall in the afternoon, while the prevailing downward motion suppresses rainfall over the SCB. At 20:00 LST in the early evening (Fig. 13b, f), the eastern TP and the western SCB are dominated by upslope winds, which is favorable for rainfall. Meanwhile, the low-level easterly deviation winds over the eastern SCB converge with the downslope winds over the eastern TP, reinforcing the upward motions over the western SCB. At 02:00 LST (Fig. 13c, g), the thermodynamic condition is almost completely reversed from the daytime. The TP becomes colder than the SCB, with downslope winds developing on its eastern slope and upward motion controlling the central and eastern SCB. In the early morning (Fig. 13d, h), the downward motion is found in almost the SCB and the whole eastern TP, together with the development of cooling before sunrise.

Comparing the diurnal variations of vertical structures of regional zonal circulation between large and small diurnal amplitude days, we can see that the vertical circulation has similar diurnal variations, but there are significant differences in magnitude. In the days of D(+)A(+), the daytime heating is crucial for driving upward motion over the eastern TP, and intense downward motion is exiting over the whole SCB (Fig. 13a). As for the days with smaller diurnal amplitude (Fig. 13e), the upward motion is stronger over the eastern slope of the TP, which is conducive to the convective activity during the day, while a weaker downward motion is observed over the SCB. In the early evening, the upward branch extends from the eastern TP to the western SCB, and the upward motion on days with large diurnal amplitude (Fig. 13b) is obviously stronger than that with small diurnal amplitude (Fig. 13f). Meanwhile, the nocturnal easterly deviation wind is evident below 700 hPa with an elevated higher equivalent potential temperature under a large diurnal amplitude condition, the warm moist flow carried by easterly deviation wind acts to intensify upward motion. The vertical circulation reverses at midnight, with more intense upward motion appears at the lower to middle troposphere over the SCB on days with large diurnal amplitude (Fig. 13c). It's worth noting that the increase of lower-tropospheric equivalent potential temperature relies heavily on the diurnal cycle of low-level winds, with the evident negative anomaly of the difference in equivalent potential temperature between 500 and 850 hPa and higher CAPE is observed over the SCB, and get strongest in the earning evening under large diurnal amplitude of low-level winds condition (Fig. S3a–d), which produces convective instability and thereby favors the nocturnal rainfall over the SCB. In contrast, the positive anomaly of the difference in equivalent potential temperature between 500 and 850 hPa and lower CAPE is distinct over the SCB throughout the day on days with small diurnal variations of low-level winds (Fig. S3m–p), which slows down the speed-up of low-level winds at night and suppresses nocturnal rainfall.

It is well recognized that daytime heating in PBL with elevated terrain can induce the diurnal changes of vertical motion, and thus characterize the regional forcing on shorter time scales. With large diurnal amplitude (Fig. 13a), the upward motion over the eastern slope of the TP is weak at 14:00 LST and corresponds to a relatively cloudless weather, which correlates with strong diabatic heating in PBL during the day. This corresponds to anomalous warming condition at low-level (Fig. 10a) and suppressed daytime rainfall (Fig. 8). Thus, such intense sensible heating in the daytime drives the diurnal circulation and contributes to the nocturnal acceleration of easterly, resulting in the enhancement of upward motion (Fig. 13b). On the contrary, stronger upward motion is observed over the eastern slope of the TP when low-level wind with a small diurnal amplitude (Fig. 13e), which benefits to the convective activity and weakens the sensible heating during the day. This feature corresponds to the large rainfall in the daytime (Fig. 8) and anomalous cooling PBL (Fig. 10b) over the SCB. Therefore, it slows down the nocturnal easterly and corresponds to a weak upward motion over the SCB. These differences suggest that the nocturnal acceleration of easterly caused by slope heating can strongly regulate the diurnal variations of upward motion over the eastern slope of the TP and the SCB.

6 Conclusions and discussion

In this study, the 21-year climatology data has been carried out to study the role of low-level winds on diurnal variations of rainfall over the SCB. Consistent with previous studies, the LLJ caused by boundary layer inertial oscillations plays an important role in controlling the diurnal cycles of rainfall during the summertime in the SCB east of the TP. The intensity of the low-level wind and its diurnal variation have an important influence on the regional characteristics of rainfall over the SCB. We further classify the low-level winds into four categories (strong or weak daily mean wind coupled with large or small diurnal amplitude) to investigate the atmospheric processes governing the rainfall over the SCB. Specific findings of this study are summarized below.

(1) More abundant rainfall is observed under strong mean wind condition, but the spatial distributions of rainfall have an evident regional discrepancy over the SCB,

which is regulated by the diurnal amplitudes of easterly. The strong mean wind with a large diurnal amplitude produces the more intense rainfall over the western SCB, corresponding to a large diurnal amplitude of rainfall peaking at midnight. On the other hand, rainfall is relatively weak and scattered on days with small diurnal amplitude. As for the weak mean wind condition, the rainfall is mostly confined to the south of the basin, and less rainfall is observed over the SCB. Moreover, a small diurnal amplitude of rainfall is observed when the daily mean wind experiences a small diurnal amplitude.

(2) The strength of the mean wind is closely related to the location of the WPSH. With a strong mean wind condition, the westward extension of the strengthening WPSH makes the low latitude southwesterly monsoon flow tunes to the southerly over the eastern YGP and transports the warm and moist air to the SCB. The southwesterlies has a weaker southerly component over the eastern YGP and the more warm and moist air is transported to the South China under a weak mean wind condition. The warmer PBL contributes greatly to the enhancement of the diurnal variation of the low-level winds, while anomalous cooling related to the deepened midlatitude trough suppresses the diurnal variations of wind. The acceleration of nocturnal easterly associated with the extended WPSH and warmer PBL results in considerable rainfall amount with pronounced diurnal variation within the basin.

(3) The strong mean wind, coupled with the evident nocturnal acceleration of low-level winds, can enhance the moisture transport and its convergence across the southeastern side of the SCB. Meanwhile, there is an intense positive anomaly of precipitable water, which contributes the formation of nocturnal rainfall over the SCB. The diurnal moisture flux convergence with a large diurnal amplitude of low-level winds increases notably from early night to midnight and peaks at about 21:00 LST. In contrast, the water vapor convergence weakens under a small diurnal amplitude of low-level winds or weak mean wind conditions.

(4) The nocturnal acceleration of low-level easterly wind caused by slope heating is crucial for driving upward motion over the eastern TP and SCB. With a large diurnal amplitude of low-level winds, the daytime upward motion over the eastern slope of the TP is weak compared to that with a small diurnal amplitude. It corresponds to a relatively cloudless weather during the day. Meanwhile, strong downward motion is observed over the SCB, suppressing the daytime rainfall. In the early night, the intense daytime heating drives the vertical circulation and contributes to the nocturnal acceleration of easterly, resulting in the enhancement of upward motion over the western SCB that favors the nighttime rainfall, but the upward motion is weak with a small diurnal amplitude of winds.

In this study, the associated cloudiness is thought to induce a relatively cold PBL and thereby a small diurnal amplitude of low-level winds. The diurnal variations of cloud regimes over the eastern TP and its relationship to the convective activities over the SCB should be considered as a key issue to reveal the possible connections of cloud and precipitation. Some studies reveal a strong coupling of clouds, radiation, winds, and rainfall over the East Asian monsoon regions and the coastal South China (Li et al. 2022a, b; Wu et al. 2023). Further studies are needed to focus on the physical processes involved in diurnal variation of cloud and precipitation processes over the eastern TP and their impact on rainfall over the SCB. This work will contribute to a better understanding of multiscale characteristics of rainfall from the perspective of cloud processes, and provide a framework for understanding the linkage from atmospheric conditions to clouds and further rainfall.

Supplementary Information The online version contains supplementary material available at https://doi.org/10.1007/s00382-023-07009-w.

Acknowledgements This work was jointly supported by the National Natural Science Foundation of China (U2142214, 42205013, 42075154, 42005039 and 42030611), the Sichuan Science and Technology Program (2022YFS0540), the Science and Technology Development Fund of Chinese Academy of Meteorological Sciences (2023KJ028) and the Open Grants of the State Key Laboratory of Severe Weather (2021LASW-A06). The authors wish to thank the National Aeronautics and Space Administration for the GPM precipitation products and the European Centre for Medium-Range Weather Forecasts for the ERA5 reanalysis data.

Author contributions Conceptualization: JL, HC. Formal Analysis: JL. Funding acquisition: JL, HC, XWJ, PL. Investigation: JL. Methodology: JL, HC. Resources: JL, HC. Supervision: HC, XJ. Writing – original draft: JL. Writing – review & editing: JL, HC, XJ, PL.

Availability of data and materials The GPM precipitation product used in this study is available at https://disc.gsfc.nasa.gov/datasets/GPM_3IMERGHH_06/summary?keywords=GPM. The ERA5 hourly reanalysis data is available at http://climate.copernicus.eu/products/climate-reanalysis.

Declarations

Conflict of interest The authors have no competing interests to declare that are relevant to the content of this article.

Ethical approval I would like to declare on behalf of my co-authors that the work described was original research that has not been published previously, and not under consideration for publication elsewhere, in whole or in part. All the authors listed have approved the submission of this work.

References

Asong ZE, Razavi S, Wheater HS, Wong JS (2017) Evaluation of Integrated Multisatellite Retrievals for GPM (IMERG) over southern Canada against ground precipitation observations: a preliminary assessment. J Hydrometeorol 18(4):1033–1050. https://doi.org/10.1175/JHM-D-16-0187.1

Bao XH, Zhang FQ, Sun JH (2011) Diurnal variations of warm-season precipitation east of the Tibetan plateau over China. Mon Weather Rev 139:2790–2810. https://doi.org/10.1175/MWR-D-11-00006.1

Blackadar AK (1957) Boundary layer wind maxima and their significance for the growth of nocturnal inversions. Bull Am Meteor Soc 38:283–290. https://doi.org/10.1175/1520-0477-38.5.283

Chen GX (2020) Diurnal cycle of the Asian summer monsoon: air pump of the second kind. J Clim 33:1747–1775. https://doi.org/10.1175/JCLI-D-19-0210.1

Chen HM, Yu RC, Li J, Yuan WH, Zhou TJ (2010) Why nocturnal long-duration rainfall presents an eastward-delayed diurnal phase of rainfall down the Yangtze River Valley. J Clim 23:905–917. https://doi.org/10.1175/2009JCLI3187.1

Chen GX, Yoshida R, Sha WM, Iwasaki T, Qin HL (2014) Convective instability associated with the eastward propagating rainfall episodes over eastern China during the warm season. J Clim 27:2331–2339. https://doi.org/10.1175/JCLI-D-13-00443.1

Chen GX, Du Y, Wen ZP (2021) Seasonal, interannual, and interdecadal variations of the East Asian summer monsoon: A diurnal-cycle perspective. J Clim 34(11):4403–4421. https://doi.org/10.1175/JCLI-D-20-0882.1

Cui CG, Zhou W, Yang H et al (2023) Analysis of the Characteristics of the Low-level Jets in the Middle Reaches of the Yangtze River during the Mei-yu Season. Adv Atmos Sci 40:711–724. https://doi.org/10.1007/s00376-022-2107-1

Curio J, Schiemannm R, Hodges KI, Turner AG (2019) Climatology of Tibetan plateau vortices in reanalysis data and a high-resolution global climate model. J Clim 32:1933–1950. https://doi.org/10.1175/JCLI-D-18-0021.1

Feng XY, Liu CH, Fan GZ, Liu XD, Feng CY (2016) Climatology and structures of southwest vortices in the NCEP climate forecast system reanalysis. J Clim 29:7675–7701. https://doi.org/10.1175/JCLI-D-15-0813.1

Fu SM, Mai Z, Sun JH, Li WL et al (2019) Impacts of convective activity over the Tibetan Plateau on plateau vortex, southwest vortex, and downstream precipitation. J Atmos Sci 76:3803–3830. https://doi.org/10.1175/JAS-D-18-0331.1

Hersbach H, Bell B, Berrisford P et al (2019) Global reanalysis: goodbye ERA-Interim, hello ERA5. ECMWF Newslett 159:17–24. https://doi.org/10.21957/vf291hehd7

Holton JR (1967) The diurnal boundary layer wind oscillation above sloping terrain. Tellus 19:199–205. https://doi.org/10.3402/tellusa.v19i2.9766

Hou AY et al (2014) The Global precipitation measurement mission. Bull Am Meteorol Soc 95:701–722. https://doi.org/10.1175/BAMS-D-13-00164.1

Hu L, Deng DF, Gao ST, Xu XD (2016) The seasonal variation of Tibetan convective systems: satellite observation. J Geophys Res Atmos 121:5512–5525. https://doi.org/10.1002/2015JD024390

Hu XL, Yuan WH, Yu RC et al (2020) The evolution process of warm season intense regional rainfall events in Yaan. Clim Dyn 54:3245–3258. https://doi.org/10.1007/s00382-020-05168-8

Huffman GJ, Bolvin DT, Braithwaite D, Hsu K, Joyce R, Xie P (2014) NASA Global Precipitation Measurement (GPM) Integrated Multi-satellitE Retrievals for GPM (IMERG) Algorithm Theoretical Basis Document (ATBD) Version 4.4, PPS. NASA/GSFC, p 30

Huffman GJ, Bolvin DT, Nelkin EJ (2015) Integrated Multi-satellitE Retrievals for GPM (IMERG) technical documentation. NASA/GSFC Code 612:47–48

Jin X, Wu TW, Li L (2013) The quasi-stationary feature of nocturnal precipitation in the Sichuan Basin and the role of the Tibetan Plateau. Clim Dyn 41:977–994. https://doi.org/10.1007/s00382-012-1521-y

Li L, Zhang RH, Wen M (2017) Genesis of southwest vortices and its relation to Tibetan Plateau vortices. Q J R Meteorol Soc 143:2556–2566. https://doi.org/10.1002/qj.3106

Li J, Li YQ, Zhao TL, Schiemann R, Muetzelfeldt M, Jiang XW (2021) Northeastward propagation of nocturnal precipitation over the Sichuan Basin. Int J Climatol 41(1):E2863–E2879. https://doi.org/10.1002/joc.6886

Li MX, Luo YL, Min M (2022a) Characteristics of pre-summer daytime cloud regimes over coastal South China from the Himawari-8 satellite. Adv Atmos Sci 39(12):2008–2023. https://doi.org/10.1007/s00376-021-1148-1

Li R, Tang SX, Shi Z, He JX, Shi WJ, Li XH (2022b) Spatial Patterns of Errors in GPM IMERG Summer Precipitation Estimates and Their Connections to Geographical Features in Complex Topographical Area. Remote Sensing 14:4789. https://doi.org/10.3390/rs14194789

Liu BQ, Chen GX, Zeng WX, Bai LQ, Qin HL (2022) Diurnal variations of southerly monsoon surge and their impacts on East Asian summer rainfall. J Clim 35(1):159–177. https://doi.org/10.1175/JCLI-D-21-0372.1

Luo YL et al (2020) Science and prediction of heavy rainfall over China: Research progress since the reform and opening-up of new China. J Meteorol Res 34:427–459. https://doi.org/10.1007/s13351-020-0006-x

Pan H, Chen GX (2019) Diurnal variations of precipitation over North China regulated by the mountain-plains solenoid and boundary-layer inertial oscillation. Adv Atmos Sci 36(8):863–884. https://doi.org/10.1007/s00376-019-8238-3

Qian TT, Zhao P, Zhang FQ, Bao XH (2015) Rainy-season precipitation over the Sichuan basin and adjacent regions in southwestern China. Mon Weather Rev 143:383–394. https://doi.org/10.1175/MWR-D-13-00158.1

Shapiro A, Fedorovich E, Rahimi S (2016) A unified theory for the Great Plains nocturnal low-level jet. J Atmos Sci 73(8):3037–3057. https://doi.org/10.1175/jas-d-15-0307.1

Stephens GL (2005) Cloud feedback in the climate system: a critical review. J Clim 18:237–273. https://doi.org/10.1175/JCLI-3243.1

Sun JH, Zhang FQ (2012) Impacts of mountain–plains solenoid on diurnal variations of rainfalls along the Mei-yu front over the east China plains. Mon Weather Rev 140(2):379–397. https://doi.org/10.1175/MWR-D-11-00041.1

Sun GH, Hu ZY, Ma YM et al (2021) Analysis of local land atmosphere coupling characteristics over Tibetan Plateau in the dry and rainy seasons using observational data and ERA5. Sci Total Environ 774:145138. https://doi.org/10.1016/j.scitotenv.2021.145138

Tang GQ, Ma YZ, Long D, Zhong LZ, Hong Y (2016) Evaluation of GPM Day-1 IMERG and TMPA version-7 legacy products over mainland China at multiple spatiotemporal scales. J Hydrometeorol 533:152–167. https://doi.org/10.1016/j.jhydrol.2015.12.008

Ueno K, Sugimoto S, Koike T, Tsutsui H, Xu XD (2011) Generation processes of mesoscale convective systems following midlatitude troughs around the Sichuan Basin. J Geophys Res Atmos 116(D2):D02104. https://doi.org/10.1029/2009JD013780

Wang JY, Yuan HL, Wang XK, Cui CG, Wang XF (2023) Impact of thermally forced circulations on the diurnal cycle of summer precipitation over the southeastern Tibetan Plateau. Geophys Res Lett 50:e2022GL100951. https://doi.org/10.1029/2022GL100951

Wu RT, Chen GX (2021) Contrasting cloud regimes and associated rainfall over the South Asian and East Asian monsoon regions. J Clim 34(9):3663–3681. https://doi.org/10.1175/JCLI-D-20-0992.1

Wu RT, Chen GX, Luo ZJ (2023) Strong coupling in diurnal variations of clouds, radiation, winds, and precipitation during the east Asian summer monsoon. J Clim 36(5):1347–1368. https://doi.org/10.1175/JCLI-D-22-0330.1

Xia RD, Luo YL, Zhang DL, Li MX, Bao XH, Sun JS (2021) On the diurnal cycle of heavy rainfall over the Sichuan Basin during 10–18 August 2020. Adv Atmos Sci 38(12):2183–2200. https://doi.org/10.1007/s00376-021-1118-7

Xu XD, Lu CG, Shi XH, Ding YH (2010) Large-scale topography of China: a factor for the seasonal progression of the Meiyu rainband? J Geophys Res Atmos 115:D02110. https://doi.org/10.1029/2009JD012444

Xue M, Luo X, Zhu KF, Sun ZQ, Fei JF (2018) The controlling role of boundary layer inertial oscillations in Meiyu frontal precipitation and its diurnal cycles over China. J Geophys Res Atmos 123:5090–5115. https://doi.org/10.1029/2018jd028368

Yu RC, Xu YP, Zhou TJ, Li J (2007a) Relation between rainfall duration and diurnal variation in the warm season precipitation over central eastern China. Geophys Res Lett 34(13):L13703. https://doi.org/10.1029/2007GL030315

Yu RC, Zhou TJ, Xiong AY, Zhu YJ, Li JM (2007b) Diurnal variations of summer precipitation over contiguous China. Geophys Res Lett 34:L01704. https://doi.org/10.1029/2006GL028129

Yu RC, Li J, Chen HM (2009) Diurnal variation of surface wind over central eastern China. Clim Dyn 33(7–8):1089–1097. https://doi.org/10.1007/s00382-008-0478-3

Yuan WH, Yu RC, Zhang MH, Lin WY, Chen HM, Li J (2012) Regimes of diurnal variation of summer rainfall over subtropical East Asia. J Clim 25:3307–3320. https://doi.org/10.1175/JCLI-D-11-00288.1

Yuan WH, Yu RC, Zhang MH, Lin W, Fu Y (2013) Diurnal cycle of summer precipitation over subtropical East Asia in CAM5. J Clim 26(10):3159–3172. https://doi.org/10.1175/JCLI-D-12-00119.1

Zeng WX, Chen GX, Du Y, Wen ZP (2019) Diurnal variations of low-level winds and precipitation response to large-scale circulations during a heavy rainfall event. Mon Weather Rev 147(11):3981–4004. https://doi.org/10.1175/MWR-D-19-0131.1

Zhang YH, Xue M, Zhu KF, Zhou BW (2019) What is the main cause of diurnal variation and nocturnal peak of summer precipitation in Sichuan Basin, China? The key role of boundary layer low-level jet inertial oscillations. J Geophys Res Atmos 124(5):2643–2664. https://doi.org/10.1029/2018JD029834

Zhao YC (2015) A study on the heavy-rain-producing mesoscale convective system associated with diurnal variation of radiation and topography in the eastern slope of the western Sichuan plateau. Meteorol Atmos Phys 127:123–146. https://doi.org/10.1007/s00703-014-0356-y

Zheng YG, Xue M, Li B, Chen J, Tao ZY (2016) Spatial characteristics of extreme rainfall over China with hourly through 24-hour accumulation periods based on national-level hourly rain gauge data. Adv Atmos Sci 33:1218–1232. https://doi.org/10.1007/s00376-016-6128-5